Scientific Research Publishing

Journal of Modern Physics, 2017, 8, 1737-1747
http://www.scirp.org/journal/jmp
ISSN Online: 2153-120X
ISSN Print: 2153-1196

Resonant Modes of One-Dimensional Metamaterial Containing Helmholtz Resonators with Point Defect

Dongbao Gao*, Xinwu Zeng, Xuanjun Liu, Kaifeng Han

Academy of Ocean Science and Engineering, National University of Defense Technology, Changsha, China
Email: *gaodongbao@nudt.edu.cn

How to cite this paper: Gao, D.B., Zeng, X.W., Liu, X.J. and Han, K.F. (2017) Resonant Modes of One-Dimensional Metamaterial Containing Helmholtz Resonators with Point Defect. *Journal of Modern Physics*, **8**, 1737-1747.
https://doi.org/10.4236/jmp.2017.810102

Received: July 17, 2017
Accepted: September 22, 2017
Published: September 25, 2017

Abstract

The metamaterial constructed by Helmholtz resonators (HR) has low-frequency acoustic forbidden bands and possesses negative mass density and effective bulk modulus at particular frequencies. The resonant modes in one-dimensional HR structure with point defect were studied using finite element method (FEM). The results show that the acoustic energy is localized between the resonant HR and the opening in the local-resonant-type gap. There is a high pressure area around the defect resonator at the frequency of defect mode. In the Bragg type gap, the energy mainly distributes in the waveguide with harmonic attenuation due to the multi-scattering. Phase opposition demonstrates the existence of negative dynamic mass density. Local negative parameter is observed in the pass band due to the defect mode. Based on further investigation of the acoustic intensity and phase distributions in the resonators corresponding to two different forbidden bands, only one local resonant mode is verified, which is different from the three-component local resonant phononics. This work will be useful for understanding the mechanisms of acoustic forbidden bands and negative parameters in the HR metamaterial, and of help for designing new functional acoustic devices.

Keywords

Helmholtz Resonator Metamaterial, Resonant Mode, Point Defect, Local Negative Parameters, Phase Distribution

1. Introduction

Helmholtz resonator (HR) is normally constructed by a large cavity with a short

neck [1]. Due to its resonance, the resonator possesses capability of low-frequency sound absorption and elimination [2]. Recently, with the increasing research on phononic crystals and acoustic metamaterials, the structure based on HRs has been reconsidered for its property of sound forbidden [3]-[8]. Furthermore, it is found that the structure possesses negative effective bulk modulus [4] and negative dynamic mass density [5] in its band gap, and therefore it is considered as a possible material to realize new functional devices of transformation acoustics [9].

Based on the different mechanisms, there are two kinds of acoustic forbidden bands in the HR metamaterial. One is called Bragg type gap (BG), which is appeared due to the Bragg scattering in the material with periodically arrayed cells [10]. The BG can only forbid the sound waves with wavelength comparable or shorter than the lattice constant. It is unpractical to control low frequency sound using this kind of metamaterial for its huge sizes. On the other hand, the second type acoustic forbidden band is brought by local resonance of HR [11], which can be called local-resonant-type gap (LRG). The LRG exists around the eigenfrequency of the resonator. As the sound wavelength corresponding to the eigenfrequency is usually some times of magnitude larger than the geometric parameters of the resonator, low frequency sound waves can be well controlled.

The band structure is much richer when defect exists [7] comparing that of perfect periodical case. Localized mode can be observed due to the coupling of the defect units and perfect units [12] [13] as well as several new gaps of BG and/or LRG. A localized mode is that, at a particular frequency, the linear free oscillations are trapped around the defect resonators and decay exponentially away from them [7]. In this case, the acoustic energy can be captured by the point defect or limited directionally transmitting along the line defect and area defect. With this character, wave-control devices can be designed [14] [15]. Recently, Fey *et al.* [8] indicated that a wide bandgap material could be get with a subwavelength collection of detuned HRs which are considered as a series of defects. However, the problem turns complicated with the increase of the number of defects.

Comparing with two- and three-dimensional metamaterials, one-dimensional (1D) systems can be calculated with higher accuracy [1] [4]. It is also understood that the results of 1D system are helpful for understanding the property of more complex cases. In previous researches, theoretical studies on the 1D HR structures were based on the theory of Bloch wave and scattering [1] [2]. However, due to its strict periodicity assumption, this method is infeasible to deal with more complicated composites with quasiperiodicity or disperiodicity. Recently, some reduced methods were developed to analyze the acoustic transmission property of the HR structure. Cheng *et al.* [5] analyzed the acoustic transmission properties of 1D HR metamterial by means of acoustic transmission line method (ATLM). Based on the interface response theory (IRT), Wang *et al.* [7] studied 1D phononic crystals containing HRs systematically, especially on the acoustic

transmission properties of structure with point defect.

So far, these studies gave more attention to the transmission property of the HR metamaterial with simplified parameters than the details inside the structure. We believe that, with full view of distribution of the oscillation modes in the structure, a clear understanding on the mechanisms about the acoustic band gaps and negative parameters can be obtained, which is useful for designing new acoustic energy concentrator and creating high pressure environment for acoustic experiments.

In practice, since the complex geometry is simplified in former theoretical methods which are unable to investigate the detailed field distribution in the structure, an accurate approach must be introduced to analyze the resonant modes property of the HR metamaterial. The Finite Element Method (FEM) is an appropriate approach to minutely study the characteristics of the acoustic field for complex structures. On the basis of FEM, the distributions of acoustic intensity and phase for different oscillation modes in the 1D metamaterial with HRs were studied in this paper. Local resonant modes were also investigated for different forbidden gaps.

2. Model and Verification of the Method

Figure 1 shows the schematic diagram of a Helmholtz resonator which is connected with a section of waveguide forming a unit cell of the metamaterial. As a numerical example, here we consider a model with 11 HR unit cells, and the 6th one is abnormal which can be considered as a defect. The overall geometric parameters are L = 0.09 m, and d_1 = 0.025 m. For the cells, the geometrical parameters of the ten perfect units are a_2 = 0.02 m, d_2 = 0.02 m, $V = a_3 \times l_3 \times d_3$ = 0.03 × 0.04 × 0.05 m^3, while the only difference for the defect unit is that d_2 = 0.04 m. The background media is water (ρ_0 = 998 kg/m^3, c_0 = 1483 m/s). Here, we analyzed the acoustic band gap structure of the metamaterial in the region of 1 - 10 kHz.

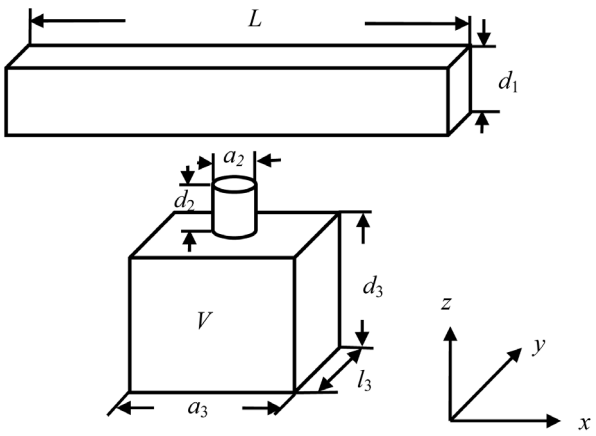

Figure 1. Schematic diagram of a Helmholtz resonator and a section of waveguide.

We studied the 3-dimensional model using COMSOL Multiphysics software (Version 4.2) which is based on the Finite Element Method (FEM). We set up the boundary conditions as shown in **Figure 2**, in which a perfect matched layer (PML) was used at the end of the waveguide to simulate the absorbing boundary condition. All the other boundaries were set to be hard walls, except that a radiation boundary condition with a harmonic wave was used as the incident wave. The host medium in the waveguide and the resonators is water.

To the computational mesh, in our simulation, at least 8 elements per wavelength were used, which guaranteed the accuracy of the method, and also satisfied the general six-element-per-wavelength rule in acoustic mesh [16]. All elements are hexahedral.

To validate the feasibility of the software using FEM, we first made a comparison between the results of FEM and ATLM [5] [17] for the acoustic transmission property of the metamaterial.

In ATLM, based on the transformation relationship between acoustic impedances of the inlet and outlet, the transmission coefficient can be obtained by applying this formula recursively.

The impedance transfer formula [16] of ATLM can be written as

$$Z_1 = Z_0 \times \frac{Z_r + jZ_0 \tan(kL)}{Z_0 + jZ_r \tan(kL)} \tag{1}$$

where, Z_1 (Z_r) is the effective impedance of the inlet (outlet) of the unit cell. $Z_0 = \rho_0 c_0 / S_g$ is the distributed impedance of the duct. S_g is the cross-section area of the waveguide. k is the wave vector of the host medium. L is the distance between two adjacent HRs.

With the assumption of long-wavelength, the transfer impedance of the waveguide parallels to the HR impedance Z_h [16]. The parallel impedance is

$$Z_c = Z_l \,||\, Z_h \tag{2}$$

which can be considered as the terminal-end impedance of its left neighbor.

By repeating this process over the N units, the effective acoustic impedance (Z_{effect}) of 1D metamaterial with N unit cells can be obtained. Then, the sound pressure reflection coefficient can be calculated as

$$r_p = \frac{Z_{\text{effect}} - Z_0}{Z_{\text{effect}} + Z_0} \tag{3}$$

The sound intensity reflection coefficient and intensity transmission coefficient are

$$r_I = \left| r_p \right|^2, \; T = 1 - r_I \tag{4}$$

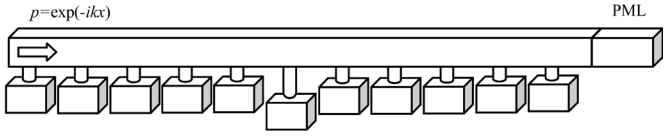

Figure 2. Finite element model of the metamterial.

In Equation (4), the band gap exists only if $T = 0$, which means $|r_p| = 1$, and therefore $Z_{\text{effect}} = 0$ or ∞. It indicates that Z_1 or/and Z_h vanishes in Equation (2). $Z_1 = 0$ corresponds to that the real and imaginary parts of Equation (1) equal zero simultaneously, which is mathematically impossible. In fact, based on Equation (1), we get that, when $KL = n\pi$, viz. $f = nc/2L$, the value of Z_1 reaches its minimum (equals to Z_r). This frequency corresponds to the central frequency of BG. On the other hand, when $Z_h = 0$, the incident wave frequency equals to the resonant frequency of the HR, which means the appearance of LRG in this case.

Figure 3 shows the acoustic transmission coefficient curves for both perfect metamaterial and structure with point defect basing on FEM and ATLM, respectively. Despite small differences, the results obtained based on FEM can also show all the properties of the HR metamaterial with point defect, such as transmission bands, forbidden bands and defect mode. Figure 3 demonstrates the feasibility of FEM, which can be a further approach to analyze the resonant

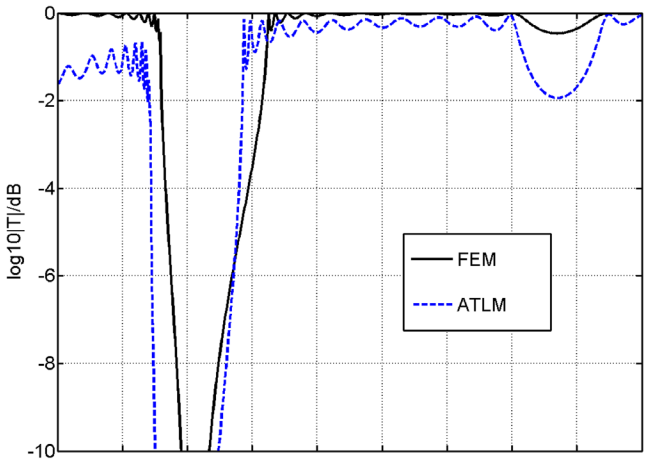

(a)

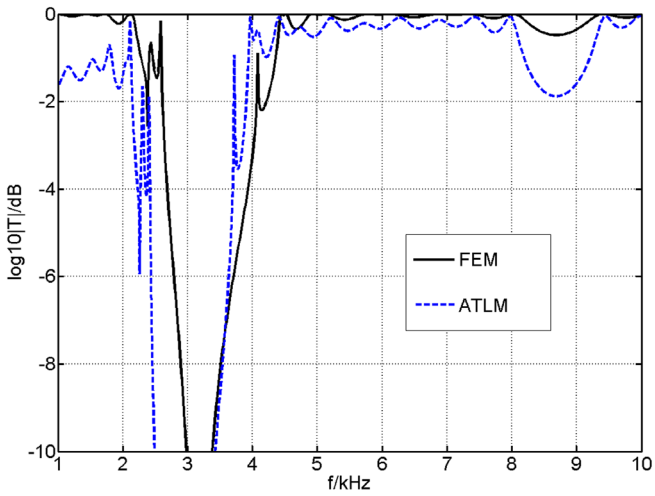

(b)

Figure 3. Comparison of acoustic transmission coefficient spectra based on FEM and ATLM for structures with (a) only perfect cells and (b) a point defect, respectively.

modes of the structure. It is also observed that the depth and width of the band calculated by FEM are much narrower and shallower than that obtained by ATLM. These characters are attributed to the inherent difference of FEM and ATLM. The main reason might be that the complex geometry of the structure is simplified by lumped parameters in ATLM, which ignores the wall effect in pipes. While in the well meshed FEM, details caused by the structure could be captured.

3. Simulation Based on FEM

Now we take a detail observation on the acoustic intensity distributions of the structure with point defect for several specified frequencies using the results with full-wave simulation based on FEM. The choice of the frequencies was based on FEM results in **Figure 3(b)**. The acoustic intensity distributions are displayed in **Figure 4**.

In **Figure 4**, point (a) locates at 1.5 kHz in the low-frequency pass band, where the acoustic intensity distributes periodically in the waveguide. Since the frequency does not reach the resonant frequency of HRs, the resonators are in the state of "pre-resonance", and the acoustic energy is being localized by the resonator. In **Figure 4(b)** (2.38 kHz), energy is localized between the defect HR and the incident opening with small amount of acoustic energy penetrating. The acoustic intensity in the waveguide is obviously weaker than that in the resonators. As we know, point (b) corresponds to the resonant frequency of the defect HR, which indicates that, in the LRG, the resonant HR can localize almost all the energy passing across it. Point (c) (2.52 kHz) is another dip between the two LRGs. Comparing with **Figure 4(b)**, the energy in the defect HR has been already released in **Figure 4(c)**. This is because that with the increase of frequency, the resonant mode of the defect HR vanishes. In this case, the sound is no

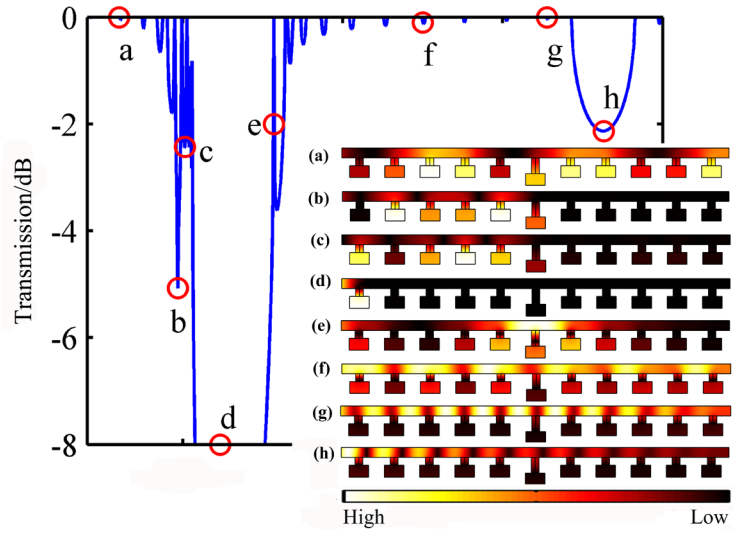

Figure 4. Acoustic pressure intensity distribution for different oscillation modes, which are corresponding to the special frequencies selected from (a) to (h), respectively.

longer localized in the resonator, and the resonators are in the state of "after-resonance". On the other hand, point (c) is also close to the resonant frequency of perfect HR. The wave oscillation in the perfect resonators becomes strong, and therefore the energy is still localized in few resonators on the incident side but released to the waveguide.

Point (d) (3.2 kHz) locates at the resonant frequency of perfect HR. In **Figure 4(d)**, almost all the acoustic energy is localized in the first HR, which further demonstrates that pressure is hold up by the first resonant HR in the LRG. In each case, a high pressure environment exists in the resonant HR, which can be helpful for acoustic energy concentrating and high-pressure experiments. However, there is a slight difference between the two resonant modes showed in **Figure 4(b)** and **Figure 4(d)**. Due to more cells resonating, the depth and width of the second LRG are larger than the first one.

Point (e) (4.08 kHz) corresponds to a defect mode, which is a narrow transmission band is the forbidden band. It is obvious that, in **Figure 4(e)**, the acoustic energy is localized around the defect HR and its neighbors. The intensity reaches the largest value at the defect resonator, and then attenuates sharply to both sides. This is a typical property of the defect mode [12]. Since the defect mode is created by the coupling of the defect HR and perfect HRs, the defect mode frequency is not the same with both resonant frequencies. The defect mode is useful for realizing new filter, energy harvester and acoustic cloaking.

Point (f) (5.1 kHz) is in the pass band outside the LRG. As shown in **Figure 4(f)**, with the increment of the pressure in the waveguide, the pressure in the HRs decreases. Now, the energy is not localized in HR, but released to the waveguide. In this case, the HRs are like obstacles to short-wavelength sound. With this conclusion, it is imaginable that the harmonicity would be more obvious and the intensity would be higher in the waveguide for **Figure 4(g)** (7.5 kHz) and (h) (8.8 kHz). Point (h) just locates in the BG. In **Figure 4(h)**, due to multi-scattering, the intensity in the waveguide attenuates gradually, which tends to zero at the terminal end. On this condition, the BG appears.

To summarize, as shown in **Figure 4**, there are plenty resonant modes in the metamterial containing HRs with point defect. When frequency is lower than the resonant frequency, the acoustic energy distributes in the waveguide and resonators symmetrically. As frequency turns to the resonant frequency, local resonant mode can localize the energy between the first resonant HR and the incident port. In the defect mode, a high pressure zone exists around the defect resonator. Finally, the energy in the resonant HR is released to the waveguide and transmits in the waveguide only when frequency is higher than the resonant frequency.

Figure 5 shows the corresponding phase distributions of **Figure 4**. In **Figure 5(a)**, the phase in the waveguide is the same as that in the shunted HR, which indicates that the resonator oscillates in-phase with the wave in the waveguide. In this case, the dynamic mass density must be positive [5] [18]. As frequency

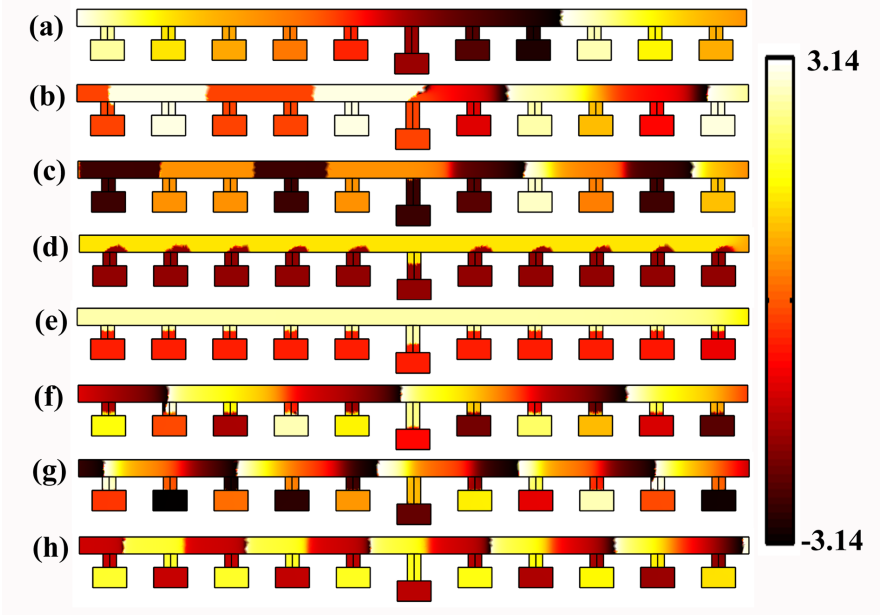

Figure 5. Phase distribution for the metamaterial containing HRs with point defect. Figures (a) to (h) correspond to the cases showed in **Figure 4**.

reaches the resonant frequency of the defect resonator (**Figure 5(b)**), though the in-phase property remains, the wave front around the defect HR is not parallel to the others due to strong oscillation of the resonant resonator. When frequency pass across the first resonant frequency (**Figure 5(c)**), a special effect must be noted that the phases between the defect HR and the waveguide are opposite, which accounts for that the local dynamic mass density becomes negative [5]. In this case, negative and positive parameters exist simultaneously in this structure.

If frequency is higher than the resonant frequency of the perfect HR (**Figure 5(d)**), the phase difference inside and outside the resonator is π. Since the HRs oscillate out of phase with the wave in the waveguide, the dynamic mass density turns negative in the whole structure. The negative parameter still exists in **Figure 5(e)**, which indicates that the negative dynamic mass density not only exists in the forbidden band, but also can be found in the pass band created by defect mode. In **Figures 5(f)-(h)**, the phase distribution in the waveguide corresponds with the property of harmonic wave.

Local resonant modes, such as energy and phase distributions, in the built-in units are typical characteristics of the local resonant phononic crystals [11]. In HR metamaterials, one unit contains only a neck and a cavity, the local resonant modes distribution in the neck and cavity indicates the basic characteristic of the structure. Therefore, we should pay attention to the intensity and phase differences between the neck and the cavity of the HR, which will be discussed below.

As shown in **Figure 6**, acoustic intensity ((a) and (b)) and phase ((c) and (d)) distributions for perfect HR in different gaps are given, in which **Figure 6(a)** and **Figure 6(c)** are at 3.2 kHz in the LRG, and (b) and (d) are at 8.8 kHz in the BG.

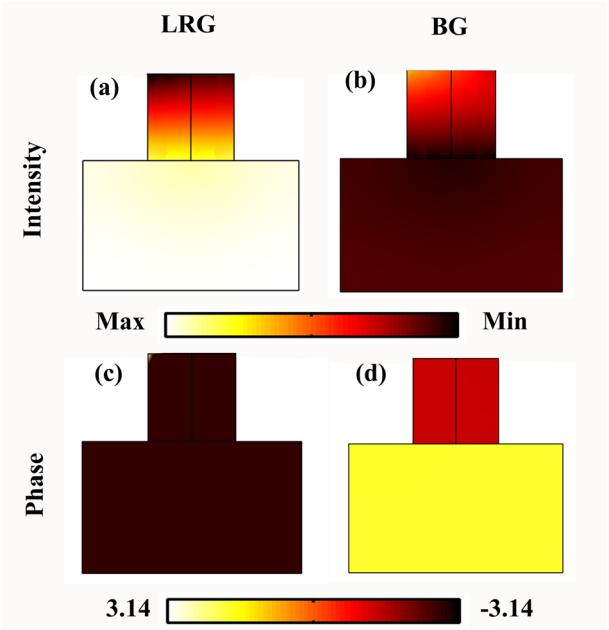

Figure 6. Acoustic intensity ((a) and (b)) and phase ((c) and (d)) distributions for Helmhotlz resonator in different forbidden bands. The frequency of (a) and (c) is 3.2 kHz corresponding to the LRG; and (b) and (d) is 8.8 kHz corresponding to the BG.

In **Figure 6(a)**, the intensity at the opening of the neck is almost zero, while that in the cavity reaches the maximum. This indicates that local resonant mode appears in the cavity, where the energy is localized. It is opposite in **Figure 6(b)**, in which the intensity in the neck is bigger than that in the cavity. However, in view of **Figure 4(h)**, we can see that the intensity in the neck is continuous with that in its connecting waveguide. Besides, in **Figure 5(h)**, the phase in the short neck is totally the same with that in the waveguide. These all indicates that there is no local resonant mode in **Figure 6(b)**. Only one kind of local resonant mode exists in the metamaterial based on Helmholtz resonators, which is different from the three-component local resonant phononics, in which two local resonant modes are discovered [19].

As shown in **Figure 6(c)**, the neck and cavity oscillate in phase. Considering with **Figure 5(d)**, it should be insisted that the negative parameter is created by both the neck and the cavity oscillating out of phase with the wave in the waveguide. If the HR oscillates strongly enough, the dynamic mass in the metamaterial can be negative. However, it is opposite in **Figure 6(d)**, where the neck oscillates out of phase with the cavity, but in phase with the wave in the waveguide (**Figure 5(h)**). In this case, only the cavity oscillates out of phase with the wave in the neck and waveguide. Therefore, the negative dynamic mass density may exist as a local parameter. Due to the energy limitation, it may not be large enough to affect the parameter of the whole structure.

4. Conclusions

To study the resonant modes in the metamaterial constructed by Helmholtz re-

sonators with point defect is useful for understanding the mechanisms of acoustic band gaps and negative parameters. The distributions of acoustic intensity and phase for 1D HR structure with point defect were analyzed basing on 3D FEM. The results show that there are different oscillation modes for different frequencies. When frequency tends to the resonant frequency of any HR, the acoustic energy is gradually localized in the resonant resonator, which results in a local-resonant-type gap. At the point of defect mode, the energy locates around the defect cell. When the wavelength is twice of the lattice, the first Bragg type gap appears, when the acoustic energy almost entirely distributes in the waveguide with harmonic attenuation. The phase distribution demonstrates that when frequency is higher than the resonant frequency, the resonant HR can oscillate out of phase with the wave in the waveguide, which is the mechanism of the negative dynamic mass density. Furthermore, the negative parameter not only exists in the forbidden band, but also can be observed in the pass band created by defect mode. Different from the typical three-component local resonant phononics, there is only one local resonant mode in one-dimensional HR metamaterial, which exists in the local resonant forbidden band. This work will be helpful for designing new functional acoustic devices.

In this paper, only two-dimensional linear problems are investigated. More complicated models are not included here. For example, we also observe that there are non-parallel interfaces of the phase distribution in **Figure 5**, which indicates that there maybe nonlinear phenomena exist. Furthermore, we will pay more attention on these problems in our next program.

Funds

The work is supported by National Natural Science Foundation of China (Grant Nos. 11504425 and 41374005).

References

[1] Sugimoto, N. and Horioka, T. (1995) *Journal of the Acoustical Society of America*, **97**, 1446. https://doi.org/10.1121/1.412085

[2] Masuda, M. and Sugimoto, N. (2005) *Journal of the Acoustical Society of America*, **118**, 113. https://doi.org/10.1121/1.1929237

[3] Hu, X.H. and Chan, C.T. (2005) *Physical Review E*, **71**, 055601(R). https://doi.org/10.1103/PhysRevE.71.055601

[4] Fang, N., Xi, D.J., Xu, J.Y., Ambat, M., Srituravanich, W., Sun, C. and Zhang, X. (2006) *Nature Materials*, **5**, 452. https://doi.org/10.1038/nmat1644

[5] Cheng, Y., Xu, J.Y. and Liu, X.J. (2008) *Physical Review B*, **77**, 045134. https://doi.org/10.1103/PhysRevB.77.045134

[6] Hu, X.H., Ho, K.M., Chan, C.T. and Zi, J. (2008) *Physical Review B*, **77**, 172301. https://doi.org/10.1103/PhysRevB.77.172301

[7] Wang, Z.G., Lee, S.H., Kim, C.K., Park, C.M., Nahm, K. and Nikitov, S.A. (2008) *Journal of Applied Physics*, **103**, 064907. https://doi.org/10.1063/1.2894914

[8] Fey, J. and Robertson, W.M. (2011) *Journal of Applied Physics*, **109**, 114903.

https://doi.org/10.1063/1.3595677

[9] Chen, H.Y. and Chan, C.T. (2010) *Journal of Physics D*: *Applied Physics*, **43**, 113001. https://doi.org/10.1088/0022-3727/43/11/113001

[10] Zhang, X., Liu, Z.Y., Mei, J. and Liu, Y.Y. (2003) *Journal of Physics*: *Condensed Matter*, **15**, 8207. https://doi.org/10.1088/0953-8984/15/49/001

[11] Liu, Z.Y., Zhang, X.X., Mao, Y.W., Zhu, Y.Y., Yang, Z.Y., Chan, C.T. and Sheng, P. (2000) *Science*, **289**, 1734. https://doi.org/10.1126/science.289.5485.1734

[12] Sigalas, M.M. (1997) *Journal of the Acoustical Society of America*, **101**, 1256. https://doi.org/10.1121/1.418156

[13] Munday, J.N., Bennett, C.B. and Robertson, W.M. (2002) *Journal of the Acoustical Society of America*, **112**, 1353. https://doi.org/10.1121/1.1497625

[14] Oudich, M. and Assouar, M.B. (2012) *Journal of Applied Physics*, **111**, Article ID: 014504. https://doi.org/10.1063/1.3673874

[15] Qiu, C.Y., Liu, Z.Y., Shi, J. and Chan, C.T. (2005) *Applied Physics Letters*, **86**, Article ID: 224105. https://doi.org/10.1063/1.1942642

[16] Kinsler, L.E., Frey, A.R., Coppens, A.B. and Sanders, J.V. (1982) Fundamentals of Acoustics. Wiley, New York.

[17] Zienkiewicz, O.Z. and Taylor, R.L. (2006) The Finite Element Method. 6th Edition, Elsevier.

[18] Mei, J., Liu, Z.Y., Wen, W.J. and Sheng, P. (2006) *Physical Review Letters*, **96**, Article ID: 024301. https://doi.org/10.1103/PhysRevLett.96.024301

[19] Wang, G., Wen, X.S., Wen, J.H., Shao, L.H. and Liu, Y.Z. (2004) *Physical Review Letters*, **93**, Article ID: 154302. https://doi.org/10.1103/PhysRevLett.93.154302